Massive MIMO channels - measurements and models

Gao, Xiang; Tufvesson, Fredrik; Edfors, Ove

Published in:
2013 Asilomar Conference on Signals, Systems and Computers

DOI:
10.1109/ACSSC.2013.6810277

2013

Document Version:
Peer reviewed version (aka post-print)

Massive MIMO channels - measurements and models

Xiang Gao, Fredrik Tufvesson, Ove Edfors
Department of Electrical and Information Technology, Lund University, Sweden
Email: {xiang.gao, fredrik.tufvesson, ove.edfors}@eit.lth.se

***Abstract*—Spatial multiplexing using Massive MIMO has been shown to have very promising properties, including large gains in spectral efficiency and several orders of magnitude lower transmit power, as compared to today's access schemes. The properties of massive MIMO have been studied mostly for theoretical channels with independent and identically distributed (i.i.d.) complex Gaussian coefficients. To efficiently evaluate massive MIMO in more realistic scenarios, we need channel models that capture important massive MIMO channel characteristics. We pursue this by analyzing measurement data from a measurement campaign in the 2.6 GHz frequency range, using a physically large array with 128 elements. Key propagation characteristics are identified from the measurements. We use the cluster-based COST 2100 MIMO channel model as a basis, and propose an extension to include those important propagation properties for massive MIMO. Statistical models of the total number of clusters, their visibility regions and visibility gains at the base station side are found based on the measurement data.**

I. Introduction

Massive MIMO, also known as very-large MIMO or large-scale antenna systems, is an emerging technology in wireless communications. With massive MIMO, we consider multi-user MIMO (MU-MIMO) where a base station is equipped with a large number (say, tens to hundreds) of antennas, and is serving several single-antenna users in the same time-frequency resource.

It has been shown both in theory and in real propagation environments that massive MIMO has very promising properties, including large gains in spectral efficiency and several orders of magnitude lower transmit power [1]–[4], as compared to conventional MIMO systems with a small number of antennas at the base station. So far, theoretical studies of massive MIMO are mostly done in channels with i.i.d. complex Gaussian coefficients. However, to efficiently evaluate such a new technique in more realistic scenarios, new channel models are needed that capture important properties of real massive MIMO propagation channels.

Unlike conventional MIMO with small and compact antenna arrays, massive MIMO with a large number of antennas can have antenna arrays that span tens to hundreds of wavelengths in space. Over this type of large arrays, the propagation channel cannot be seen as wide-sense stationary (WSS) as is usually the case for conventional small MIMO. This has been observed in measured channels using a 128-element linear array, as reported in [5] and [6]. When we resolve the propagation channel into scatterers, we observe that some scatterers are not visible over the whole array, and for scatterers being visible over the whole array, their power contribution may vary considerably. Thus, large-scale/shadow fading can be experienced over this large array. The power variation caused by the large-scale/shadow fading over the antenna array can be critical to performance evaluation and algorithm design for massive MIMO. Therefore, it is important to model the non-WSS characteristic of the propagation channel over the array and include it in new channel models.

We start from a well-known MIMO channel model - the COST 2100 model [7], in which only small and compact MIMO arrays have been considered so far. Based on channel measurements using the 128-element linear array, we identify propagation properties of massive MIMO channels that are missing in the COST 2100 model. Then we propose an extension to include these massive MIMO properties. These propagation properties are also modeled statistically, using the measurement data.

The rest of the paper is organized as follows. In Sec. II, we give a brief introduction on the COST 2100 MIMO channel model. In Sec. III, we describe our massive MIMO channel measurements, measurement data processing, and propagation properties that are observed from the measured channels. Then in Sec. IV we propose an extension of the COST 2100 model to include massive MIMO channel characteristics. Finally we summarize this modeling work in Sec. V.

II. COST 2100 MIMO channel model

The COST 2100 MIMO channel model is a geometry-based stochastic channel model (GSCM) that can reproduce the stochastic properties of MIMO channels over time, frequency, and space. It characterizes and models the radio channel in delay and directional domains, through the geometric distribution of scatterers, or clusters, *i.e.*, groups of multipath components (MPCs), in the propagation environment. This cluster-based channel model describes the physical channel and is antenna-independent. The directional domain, when combined with antenna array responses at transmit and receive side, can be directly transformed into the spatial dimension for wideband MIMO channel simulations.

One advantage of cluster-based channel models is that they model the time-variant/spatially-variant nature of the radio channels. In the COST 2100 model, this is done by introducing cluster visibility regions, as one of the key modeling concepts. A visibility region (VR) is a region on the azimuth plane in the simulation area, which determines the visibility of a particular cluster. Each cluster is associated with at least one VR. When a mobile enters a VR, the related cluster becomes "visible", and contributes scattering through the corresponding MPCs in the radio channel between the mobile and the base station.

The power level is controlled by a function called visibility gain, which describes the power variation of the scattering contribution within a VR. The mobile can be located in an area where multiple VRs overlap, and in this case, multiple clusters are "visible" simultaneously. The VRs are assumed to be uniformly distributed in the simulation area. When a mobile moves in the simulation area, it enters and leaves different cluster VRs. In this way, the time-variation/spatial-variation of the channel due to the movement is modeled by the variation of scattering contribution from different clusters. In the current COST 2100 model, the cluster VRs are only used at the mobile side, since the mobile terminal movement is one of the main causes of temporal and spatial variations of the channels. However, for a massive MIMO base station, when the antenna array becomes physically much larger than today's small and compact arrays, the effect of a spatially-variant channel can be experienced, but now over the large antenna array at the base station. This is shown and discussed when we analyze channel measurements in Sec. III.

More details on the COST 2100 MIMO channel model, such as general structure, parameterization, implementation and validation, can be found in [7]–[9].

III. Channel Measurements and Processing

In order to characterize and model massive MIMO channels, measurements with a large virtual array were performed. Since the cluster-based COST 2100 channel model is our modeling basis, we extract clusters from the measured channels and investigate the channel behavior of massive MIMO at a cluster level. Comparing with conventional small MIMO channels, we identify missing properties of massive MIMO in the current model. Channel measurements, measurement data processing, and observed channel behavior are presented in the following.

A. Channel measurements

The measurements were carried out outdoors around the E-building of the Faculty of Engineering (LTH), Lund University, Sweden. An overview of the semi-urban measurement area is shown in Fig. 1 (left). The base station (receive) antenna array was placed on the roof of E-building. It is a 128-element virtual linear array and spans 7.4 m in space. The distance between adjacent antenna element positions is half a wavelength at 2.6 GHz. Fig. 1 (upper and lower right) shows this physically large array with an omni-directional antenna moving on a rail, giving 128 antenna positions. At the user (transmit) side, an omni-directional antenna was moved around 8 measurement sites (MS) acting as single-antenna users. Among these sites, three (MS 1-3) have line-of-sight (LOS) conditions, and five (MS 4-8) have non-line-of-sight (NLOS) conditions. At each site, 5 positions were measured.

The measurement data were recorded at a center frequency of 2.6 GHz and a signal bandwidth of 50 MHz, using an HP 8720C vector network analyzer. With the virtual linear array and vector network analyzer, it takes around half an hour to record one measurement, *i.e.*, at the base station, the omni-directional antenna moves from the beginning of the array to the end. In order to keep the channel as static as possible during one measurement, this campaign was performed during the night when there were few objects, e.g., people and cars, moving around in the measurement area.

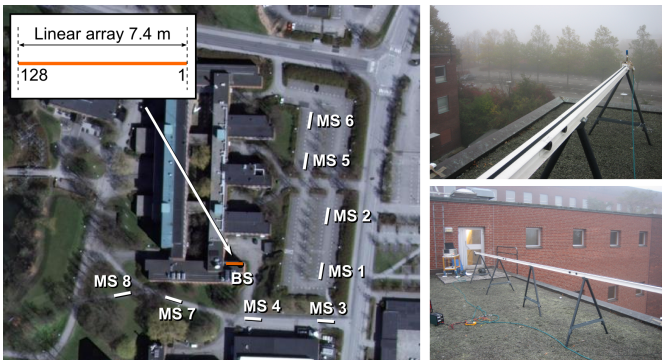

Fig. 1. Left: overview of the measurement area at the campus of the Faculty of Engineering (LTH), Lund University, Sweden. A 128-element virtual linear array at the base station was placed on the roof of the E-building. 8 measurement sites (MS 1-8) around the E-building were measured. Upper right: an omni-directional antenna moving along a rail, forms the virtual linear array with 128 equidistant antenna positions. Lower right: another view of the same virtual linear array spanning 7.4 m.

B. Measurement data processing

From the raw measurement data, *i.e.*, the channel transfer functions, we need to investigate the massive MIMO channel behavior at a cluster level and identify propagation properties that are missing in the current model. For each measured position, in order to extract the clusters in the channel, we apply a sliding window with 10 neighboring antennas over the array. From the raw measurement data within each window, we estimate the MPCs with parameters of delay, angle of arrival (AoA) in azimuth and complex amplitude, through the space-alternating generalized expectation maximization (SAGE) algorithm [10]. Based on the estimated MPC parameters, joint clustering and tracking [11] is performed. Clusters are identified by grouping the MPCs through the Kpower-Means clustering algorithm [12] for each 10-antenna window, then the identified clusters are tracked over windows along the array. The reason we process the channel data based on 10-antenna windows is that the channel can be considered as wide-sense stationary (WSS) within such window. On the basis of these WSS sub-channels, we can study the spatial-variation of the whole channel over the array. Furthermore, when the SAGE algorithm estimates the directional information[1], 10 antennas can provide relatively high angular resolution.

Through the above processing of raw measurement data, we can investigate the channel behavior at a cluster level. Angular power spectrum from the SAGE estimates and corresponding cluster power variations over the array from joint clustering and tracking are shown in Fig. 2 as examples. Fig. 2(a) and 2(b) show the angular power spectrum over the array in one LOS scenario and one NLOS scenario, respectively. From here we can see the spatial-variation of the channel over the

[1]The range of directional estimation is 0-180 degrees for the linear array. This is due to the directional ambiguity problem inherent in this type of array structure [13], thus it does not affect the channel modeling for it.

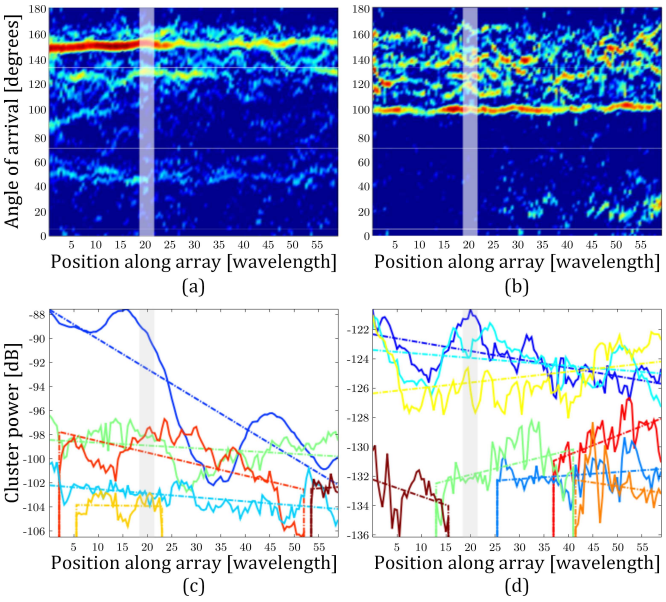

Fig. 2. Angular power spectrum and cluster power variations over the large array at the base station. (a) and (c) are results from a LOS scenario when the user is at MS 3. (b) and (d) are results from a NLOS scenario when the user is at MS 7. For the cluster power variations shown in (c) and (d), different clusters are indicated by different colors, and the solid lines are the cluster power variations over the array, which are fitted by linear slopes, *i.e.*, the dashed lines, in a least-squares sense. The shadowed regions in the four plots show examples of the channels that a conventional small MIMO array extending over a few wavelengths would experience.

large array. For example, in Fig. 2(a), the LOS component from around 150 degrees is stronger at the beginning of the array and becomes shadowed at the end of array. The power contribution from 130 degrees only appears over a part of the array. In the NLOS scenario shown in Fig. 2(b), we can see that the scattering is more rich and many scatterers are only visible over a part of the array. The corresponding cluster power variations over the array in these two scenarios are shown in Fig. 2(c) and 2(d) (solid lines). Along with the cluster power variations, we can also see the distance along the array that each cluster is visible. Some clusters are visible over the whole array, while others are only visible for a part of the array. The above shows that the massive MIMO channel cannot be considered wide-sense stationary over the large array, and thus large-scale/shadow fading is experienced.

In comparison with massive MIMO with a large array, the shadowed regions in Fig. 2 indicate a channel that a conventional small MIMO would experience. A small and compact array which spans only a few wavelengths in space would experience a very small part of the channel that a large array sees. From the shadowed regions in Fig. 2, we can see that the small MIMO channels do not have much spatial-variation: within the indicated range of the small array, the same clusters are visible and the cluster power has small variations.

IV. Modeling for Large Array

From the observation of measured channel behavior discussed above, we know that massive MIMO channels can have significant spatial-variation over the large array. To extend the

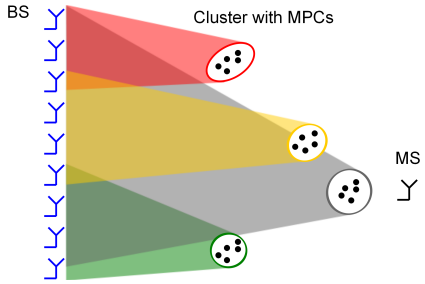

Fig. 3. Extension of the concept of cluster visibility regions to the base station side. Each antenna sign represents a small MIMO array.

current COST 2100 model to support large arrays, this spatial-variation at the base station side needs to be modeled and included. A simple way for this is to extend the concept of cluster visibility regions, as discussed in Sec. II, to the base station side. The idea is that each cluster should have two types of VRs, one at mobile station side (MS-VR), and one at base station side (BS-VR). Similar to how a mobile terminal moves in and out of MS-VRs on the mobile side, antenna elements along the large array are either inside or outside BS-VRs at the base station side. This is illustrated in Fig. 3, where colored regions imply visibility of different clusters along a large linear array.

After introducing the concept of cluster VRs on the base station side, we determine what needs to be modeled in the extension to include massive MIMO. First of all, the total number of clusters that are visible over a large array should be modeled. As can be seen from Fig. 2 and Fig. 3, more clusters are visible for a large array as compared to a small array, so the number of clusters in the current model is not suitable any more. Then, for each cluster, we assign BS-VR to it together with MS-VR, we therefore need to model the properties of BS-VRs, such as shape and size. It should be mentioned that the modeling of MS-VR in the current model cannot be directly used for BS-VR. This is because the mobile station and the base station usually have very different propagation environments in their vicinity. Mobile stations are usually moving on ground, while base stations are typically positioned on top of buildings. Another thing that should be taken into account is the cluster power variations within the BS-VRs. In the current model, the average power contribution of a cluster depends on the geometry of the cluster location in the simulated propagation environment. As an extension, what we need to model here is only the variation of cluster power, which is the cluster visibility gain at the base station side.

The modeling of the total number of clusters, cluster visibility region and visibility gain at the base station side are discussed in the following. We model them statistically based on the processed measurement data. As being done for the current model in [8], LOS and NLOS scenarios are modeled and parameterized separately, since they show different statistics from the measurement data. Here we show the modeling and parameterization for NLOS scenarios, based on the measurements at MS 4-8 (see Fig. 1), as an example. For LOS scenarios, the modeling and parameterization are done in the same way, but result in different values on the

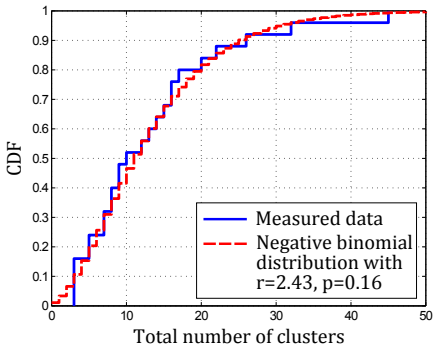

Fig. 4. CDF of the total number of clusters, which is modeled as negative binomial distribution with the estimated parameters $r = 2.43$ and $\sigma = 0.16$.

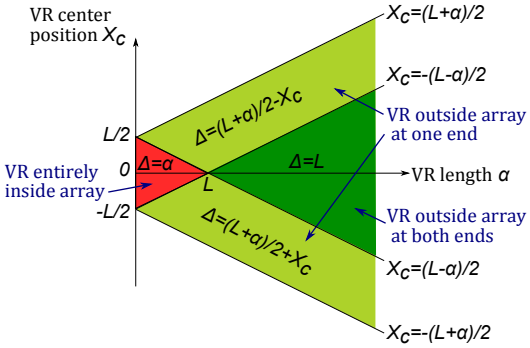

Fig. 5. Illustration of the relationship between a cluster's true BS-VR length α and observed BS-VR length on the array Δ, depending on the BS-VR center position X_c. On the axis of BS-VR center position, the origin is at the center of the linear array, and L represents the length of the array.

estimated distribution parameters.

A. Total number of clusters

Fig. 4 shows the statistics of the total number of clusters that are visible in the range of 7.4 m linear array in the NLOS scenarios. Since the data can only take on discrete values, we use a negative binomial distribution to model it, as can be seen in Fig. 4. The two parameters of the negative binomial distribution are obtained through maximum-likelihood estimation (MLE). Note that the clusters are extracted from the channel when the mobile is at one measurement position. It means that only clusters with MS-VRs overlapping that position are visible. If the movement of mobile station is considered, the total number of clusters in the environment should be even higher than what we observe in this measurement.

B. Cluster visibility region at the base station side

In the current model, the MS-VRs are modeled as circular regions of a fixed size. However, a modification has been suggested in [8] to introduce variations in the VR size. In contrast to the MS-VRs which are two-dimensional regions on the azimuth plane, the BS-VRs have to be modeled as intervals for now, since the large linear array only spans one dimension. The lengths of these intervals are the BS-VR sizes, for which the modeling is discussed in the following.

As can be seen in Fig. 2, some clusters have BS-VRs entirely inside the array, and some clusters have BS-VRs that overlap one or both ends of the array. For the former case, the observed BS-VR length on the array is the cluster's true BS-VR length, while for the latter case, the true BS-VR length may be much longer than what is observed on the array. Since the physical size of the linear array is limited, we can only measure part of the length of many cluster BS-VRs. In order to model the true BS-VR lengths from the observed data, we derive the relationship between the true BS-VR length and the observed BS-VR length, depending on the BS-VR center position along the array. This relationship is illustrated in Fig. 5. For the three cases of the BS-VR being entirely inside the array, outside the array at one end and outside the array at both ends, we can write the observed BS-VR length Δ as a function of the true length α and the center position X_c. We assume that the cluster BS-VR center positions X_c are uniformly distributed along the line of the array in space, just as in the current model the MS-VRs are uniformly distributed in the simulation area. Then we can find the relationship between the distributions of Δ and α. The cumulative distribution function (CDF) of the observed BS-VR lengths, $K_\Delta(y)$, can be written as a function of the probability density function (PDF) of the true BS-VR lengths, $f_\alpha(\nu)$, as

$$K_\Delta(y) = \begin{cases} K'_\Delta(y), & y \le L \\ 1, & y > L, \end{cases} \tag{1}$$

where

$$\begin{aligned} K'_\Delta(y) = &\int_{\Delta_0}^{y} f_\alpha(\nu)\mathrm{d}\nu + 2y\int_{y}^{\infty} \frac{1}{L+\nu} f_\alpha(\nu)\mathrm{d}\nu \\ &- 2\Delta_0 \int_{\Delta_0}^{\infty} \frac{1}{L+\nu} f_\alpha(\nu)\mathrm{d}\nu, \end{aligned} \tag{2}$$

L is the length of the array, and Δ_0 is the smallest observation of the BS-VR length on the array due to measurement data processing.

Having the relationship of the distributions of the observed BS-VR lengths and the true BS-VR lengths above, we can assume any particular distribution of the true BS-VR lengths, *i.e.*, $f_\alpha(\nu)$, and find its parameters through an MLE approach based on the observed data. Here we select a log-normal distribution, judging from the shape of the empirical distribution seen in the measurements, and estimate its two parameters. The estimation result is shown in Fig. 6(a), where the true BS-VR length follows log-normal distribution with the estimated parameters. We can also see the fitting of the distribution of observed BS-VR lengths from the MLE result to the measured data, as shown in Fig. 6(b) and Fig. 6(c). Fig. 6(c) shows the data of BS-VR entirely inside the array and the data of BS-VR outside the array separately. We can see that for the part that BS-VRs are entirely inside the array, the MLE result fits quite well, while for the part that BS-VRs are outside the array, the MLE fitting in the CDF plot is slightly higher than the measured data. Despite this, we can see in Fig. 6(b) the MLE fitting is quite good for the whole data set.

C. Cluster visibility gain at the base station side

For the cluster power variations within the BS-VRs, since the small-scale fading has already been modeled as the con-

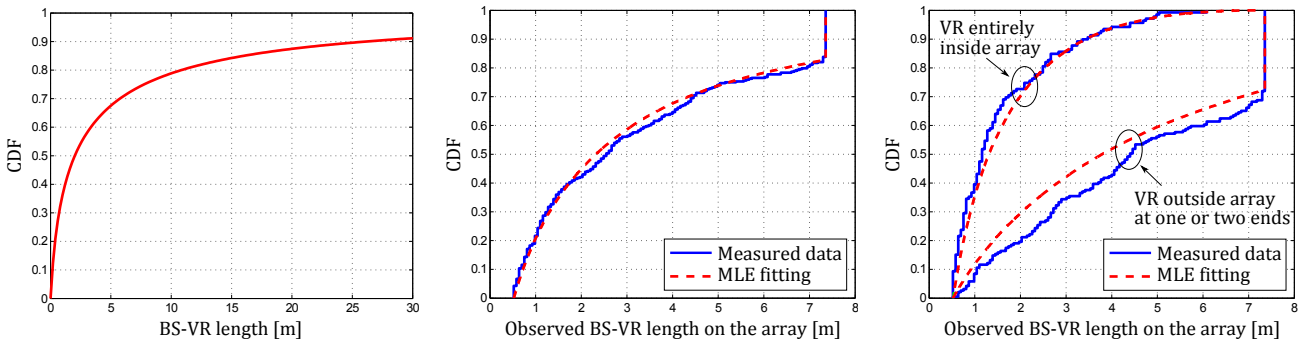

(a) (b) (c)

Fig. 6. Distributions of the true BS-VR lengths and observed BS-VR lengths on the array. (a) CDF of the estimated true BS-VR lengths, which follows a log-normal distribution with the estimated parameters of logarithm mean $\mu = 0.7$ and logarithm standard deviation $\sigma = 2$. (b) CDF of the observed BS-VR lengths on the array and the fitting through the MLE approach. (c) CDFs of the observed BS-VR lengths and the fittings through the MLE approach, splitting into two groups: BS-VRs entirely inside the array and BS-VRs outside the array at one or both ends.

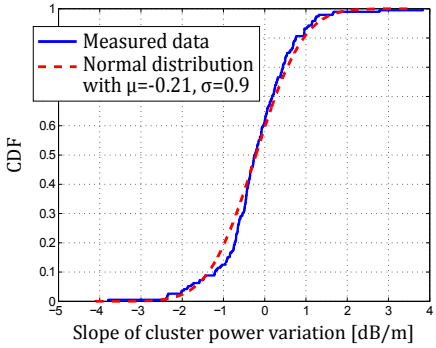

Fig. 7. CDF of the slopes of cluster power variations in their BS-VRs. It follows normal distribution with the estimated parameters of the mean $\mu = -0.21$ and the standard deviation $\sigma = 0.9$.

structive and destructive effects of the MPCs in the current model, what we need to capture here is the large-scale fading along the array. For simplicity, we use linear slopes in dB to fit the cluster power variations, as shown in the dashed lines in Fig. 2(c) and (d). These linear slopes are estimated in a least-squares sense in the dB domain. The CDF of the slopes of these linear changes in dB are shown in Fig. 7. Note that for clusters with small observed BS-VRs, the estimation of the slopes may be unreliable. Thus in Fig. 7, the slopes for the clusters with observed BS-VRs larger than 25 windows, *i.e.*, about 2 m, are shown and fitted well by the normal distribution.

V. Summary

In this paper, the ongoing work of cluster-based modeling for massive MIMO channel is presented. We start from the well-known COST 2100 MIMO channel model, in which only small and compact MIMO arrays have been considered so far. Based on channel measurements using a physically large array with 128 elements, we have studied the massive MIMO channel behavior and identified important propagation properties missing in the current COST 2100 model. The observation is that the channel cannot be seen as wide-sense stationary over the large array at the base station. Therefore, an extension of the current model to support large arrays is proposed. The concept of cluster visibility regions in the current model is extended to the base station side to model the spatial-variation of the channel over the large array. Then statistical models of the total number of clusters, their visibility regions and visibility gains at the base station side are found based on the measured data.

References

[1] F. Rusek, D. Persson, B. K. Lau, E. G. Larsson, T. L. Marzetta, O. Edfors, and F. Tufvesson, "Scaling up MIMO: Opportunities and challenges with very large arrays," *IEEE Signal Processing Magazine*, Jan. 2013.

[2] E. G. Larsson, F. Tufvesson, O. Edfors, and T. L. Marzetta, "Massive MIMO for next generation wireless systems," *CoRR*, vol. abs/1304.6690, 2013.

[3] H. Q. Ngo, E. G. Larsson, and T. L. Marzetta, "Energy and spectral efficiency of very large multiuser MIMO systems," *IEEE Transactions on Communications*, vol. 61, no. 4, pp. 1436–1449, 2013.

[4] X. Gao, F. Tufvesson, O. Edfors, and F. Rusek, "Measured propagation characteristics for very-large MIMO at 2.6 GHz," in *2012 4th Asilomar Conference on Signals, Systems and Computers (ASILOMAR)*, 2012, pp. 295–299.

[5] S. Payami and F. Tufvesson, "Channel measurements and analysis for very large array systems at 2.6 GHz," in *2012 6th European Conference on Antennas and Propagation (EUCAP)*, Mar. 2012, pp. 433–437.

[6] X. Gao, F. Tufvesson, O. Edfors, and F. Rusek, "Channel behavior for very-large MIMO systems - initial characterization," in *COST IC1004, Bristol, UK*, Sep. 2012.

[7] L. Liu, C. Oestges, J. Poutanen, K. Haneda, P. Vainikainen, F. Quitin, F. Tufvesson, and P. Doncker, "The COST 2100 MIMO channel model," *IEEE Wireless Communications*, vol. 19, no. 6, pp. 92–99, 2012.

[8] M. Zhu, G. Eriksson, and F. Tufvesson, "The COST 2100 channel model: Parameterization and validation based on outdoor MIMO measurements at 300 mhz," *IEEE Transactions on Wireless Communications*, vol. 12, no. 2, pp. 888–897, 2013.

[9] R. Verdone and A. Zanella, *Pervasive Mobile and Ambient Wireless Communications: COST Action 2100*. Springer, 2012.

[10] B. Fleury, M. Tschudin, R. Heddergott, D. Dahlhaus, and K. Ingeman Pedersen, "Channel parameter estimation in mobile radio environments using the SAGE algorithm," *IEEE Journal on Selected Areas in Communications*, vol. 17, no. 3, pp. 434–450, Mar. 1999.

[11] N. Czink, *The Random-Cluster Model - A Stochastic MIMO Channel Model for Broadband Wireless Communication Systems of the 3rd Generation and Beyond*. Dissertation, Telecommunications Research Center Vienna (FTW), 2007.

[12] N. Czink, P. Cera, J. Salo, E. Bonek, J.-P. Nuutinen, and J. Ylitalo, "A framework for automatic clustering of parametric MIMO channel data including path powers," in *Vehicular Technology Conference, 2006. VTC-2006 Fall. 2006 IEEE 64th*, Sep. 2006, pp. 1–5.

[13] A. Manikas and C. Proukakis, "Modeling and estimation of ambiguities in linear arrays," *IEEE Transactions on Signal Processing*, vol. 46, no. 8, pp. 2166–2179, 1998.